AD-A107 038 COLD REGIONS RESEARCH AND ENGINEERING LAB HANOVER NH F/G 8/12
A MACROSCOPIC VIEW OF SNOW DEFORMATION UNDER A VEHICLE.(U)
JUL 81 P W RICHMOND, G L BLAISDELL
UNCLASSIFIED CRREL-SR-81-17 NL

END
DATE FILMED
12-81
DTIC

Special Report 81-17

July 1981

(12) LEVEL II

A MACROSCOPIC VIEW OF SNOW DEFORMATION UNDER A VEHICLE

Paul W. Richmond and George L. Blaisdell

Prepared for
DIRECTORATE OF MILITARY PROGRAMS
OFFICE OF THE CHIEF OF ENGINEERS
By

UNITED STATES ARMY CORPS OF ENGINEERS
COLD REGIONS RESEARCH AND ENGINEERING LABORATORY
HANOVER, NEW HAMPSHIRE, U.S.A.

Approved for public release; distribution unlimited.

Unclassified

SECURITY CLASSIFICATION OF THIS PAGE (When Data Entered)

REPORT DOCUMENTATION PAGE		READ INSTRUCTIONS BEFORE COMPLETING FORM
1. REPORT NUMBER Special Report 81-17	2. GOVT ACCESSION NO. AD-A107	3. RECIPIENT'S CATALOG NUMBER 038
4. TITLE (and Subtitle) A MACROSCOPIC VIEW OF SNOW DEFORMATION UNDER A VEHICLE		5. TYPE OF REPORT & PERIOD COVERED 6. PERFORMING ORG. REPORT NUMBER
7. AUTHOR(s) Paul W. Richmond and George L. Blaisdell		8. CONTRACT OR GRANT NUMBER(s)
9. PERFORMING ORGANIZATION NAME AND ADDRESS U.S. Army Cold Regions Research and Engineering Laboratory Hanover, New Hamphire 03755		10. PROGRAM ELEMENT, PROJECT, TASK AREA & WORK UNIT NUMBERS DA Project 4A762730AT42, Technical Area A, Work Unit 015
11. CONTROLLING OFFICE NAME AND ADDRESS Directorate of Military Programs Office, Chief of Engineers Washington, D.C. 20314		12. REPORT DATE July 1981 13. NUMBER OF PAGES 25
14. MONITORING AGENCY NAME & ADDRESS(if different from Controlling Office) CRREL-SR-81-17		15. SECURITY CLASS. (of this report) Unclassified 15a. DECLASSIFICATION/DOWNGRADING SCHEDULE

16. DISTRIBUTION STATEMENT (of this Report)

Approved for public release; distribution unlimited.

17. DISTRIBUTION STATEMENT (of the abstract entered in Block 20, if different from Report)

18. SUPPLEMENTARY NOTES

19. KEY WORDS (Continue on reverse side if necessary and identify by block number)

Ground traffic
Mobility
Snow
Stress tests

20. ABSTRACT (Continue on reverse side if necessary and identify by block number)

In this report the deformation of snow under a vehicle is discussed. For snow with an initial density of less than 0.45 Mg/m^3, load transfer through shallow snow is shown to be attenuated by an interfacial boundary force. Evidence is presented that shows the existence of a density distribution in the deformed area. Results of a laboratory plate-sinkage test on sintered snow support this analysis. Maximum values obtained for the interfacial boundary force range from 1335 to 2670 N when the average density of the deformed area is about 0.5 Mg/m^3..

DD FORM 1 JAN 73 1473 EDITION OF 1 NOV 65 IS OBSOLETE

Unclassified

SECURITY CLASSIFICATION OF THIS PAGE (When Data Entered)

037200

PREFACE

This report was prepared by Paul W. Richmond, Mechanical Engineer, and George L. Blaisdell, Research Civil Engineer, of the Applied Research Branch, Experimental Engineering Division, U.S. Army Cold Regions Research and Engineering Laboratory. This study was funded under DA Project 4A762730AT42, Design, Construction and Operations Technology for Cold Regions, Technical Area A, Combat Operations Support, Work Unit 015, Mine/Countermine Performance in Cold Environments.

The authors thank Dr. R. Liston and G. Abele of CRREL for their technical review of the report.

CONTENTS

ILLUSTRATIONS

TABLES

A MACROSCOPIC VIEW OF SNOW DEFORMATION UNDER A VEHICLE

by

Paul W. Richmond
George L. Blaisdell

INTRODUCTION

The study of snow deformation under a vehicle is applicable to two areas of winter warfare: vehicle mobility and mine warfare. Considerable research has been performed in the area of vehicle mobility, but little work has been done relative to mine warfare under winter conditions. During World War II it was observed that a snow cover could render a pressure mine ineffective due to attenuation of the vehicle load through the snow (Gensler 1973). Emplacement procedures for installing mines in snow have been developed, but no work has been done to explain the load attenuation mechanism.

In this report the deformation and load attenuation of snow under a vehicle is discussed and results of laboratory plate-sinkage tests are presented. The results and observations made during the discussion of snow deformation are applied in general to vehicle mobility and land mines.

DEFORMATION OF SNOW UNDER A VEHICLE

A vehicle traveling over dry snow exerts a load which compresses the snow under its wheels or tracks, thus forming a rut. If the snow is excavated so that the cross section can be observed, a nearly rectangular deformed area will be found (Fig. 1). A review of related literature reveals that this observation is limited to snow covers with initial densities of about 0.45 Mg/m^3 or less. For higher density snow Wuori (1962) and Abele (1970) present data that show a deformation pattern similar to that described by the typical Boussinesq stress bulb. Figure 1 indicates that the majority of deformation occurs vertically, although some deformation may also occur horizontally in front of the compacting element. For convenience it will be assumed that horizontal deformation affects only motion resistance (see Blaisdell in prep.) thus limiting the topic of the discussion to vertical deformation. It is also assumed that the duration of the applied load is short enough to avoid any effects of creep.

Figure 1. Cross section of area deformed by vehicle (Harrison 1975).

In mobility research, two types of snow have been defined: deep and shallow. The difference between them, as illustrated in Figure 2, is that in deep snow an undisturbed layer exists between the deformed snow and the underlying surface.

Figure 3 is a simple free body diagram that identifies the forces acting on the deformed snow mass. In the static condition depicted, the load L must equal the sum of the other two forces, or

$$L = T + S. \qquad (1)$$

The shearing force S is the result of interfacial friction. In shallow snow, T is the force transferred to the underlying rigid surface. For deep snow, T must be equal to the yield strength of the snow, which in most cases can be considered negligible. Vehicle sinkage and subsequent growth of the deformed area must continue until the sum of S and T equals the applied load.

Force (load) vs sinkage curves of in-situ snow have typically been obtained using a bevameter; a simple schematic of this force-sinkage device is shown in Figure 4. Continuous measurements of force and sinkage are made with the bevameter and representative data obtained by Bennett (1973)

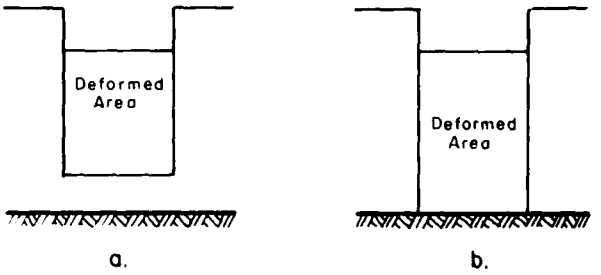

Figure 2. Deep (a) and shallow (b) snow.

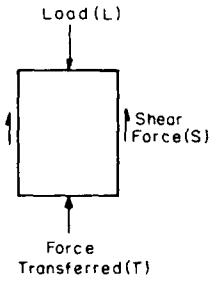

Figure 3. Free body diagram of deformed area.

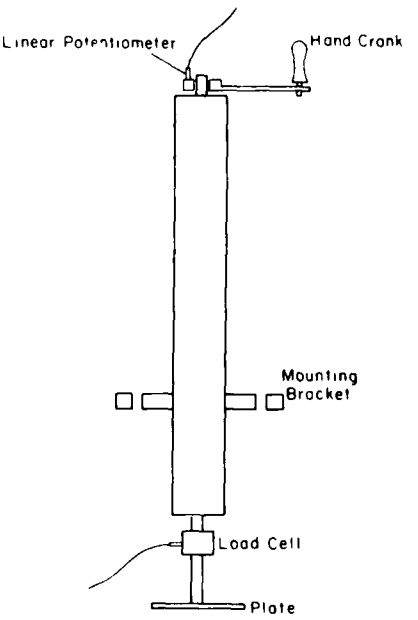

Figure 4. Schematic of bevameter.

are shown in Figure 5. Laboratory tests have been conducted by Abele (1970) and others using grids painted on a snow surface to measure the depth of deformation (Fig. 6). Examination of this type of data produced the representative schematic depicted in Figure 7.

The horizontal lines in Figure 7a represent the location of snow crystals after deformation. The absence of deformation below point d indicates that the stress at this point must be lower than or equal to the yield strength of the snow at this depth. Examination of the relative location of the deformation lines suggests that post-compaction densities decrease with depth, as becomes apparent by calculating the area change

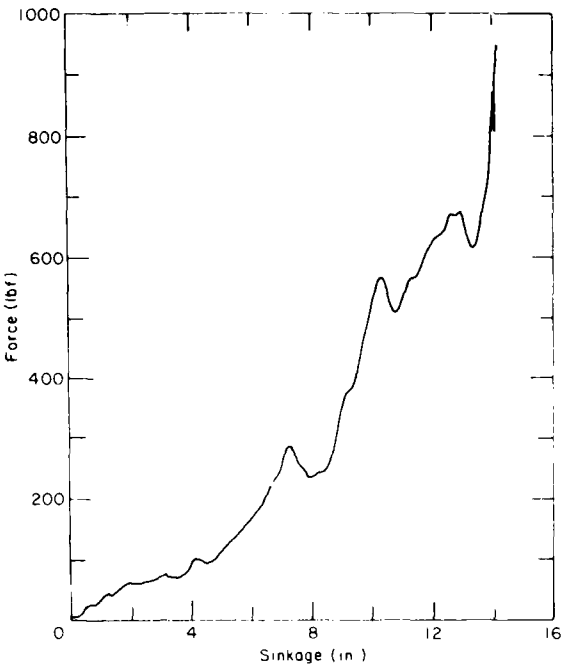

Figure 5. Representative data obtained from bevameter (Bennett 1973).

between these lines. With this technique, results from laboratory tests discussed below were used to generate an approximate density vs depth curve (Fig. 7b). The critical density is the maximum density obtainable by vehicle compaction and is generally reported to be about 0.5 Mg/m^3. This agrees with the results shown in Figure 7b.

If a load is applied so that the deformed area extends to the base of the snow cover, the shallow snow case is observed. Any increase in load above that required to extend to the rigid base results in an increase in the force T (eq 1). Data presented below indicate that S also increases due to the increasing force normal to the interface. This increase in S offsets any decrease due to the area change. With increasing load, deformation continues until the entire deformation area is at the critical density (assuming the underlying surface does not deform). At this point, an equation relating the snow depth h, initial snow density γ_o, critical density γ_{cr} and the effective sinkage or maximum rut depth z_e can be written; Harrison (1975b) has presented this relationship as

$$z_e = h\ (1 - \frac{\gamma_o}{\gamma_{cr}}). \qquad (2)$$

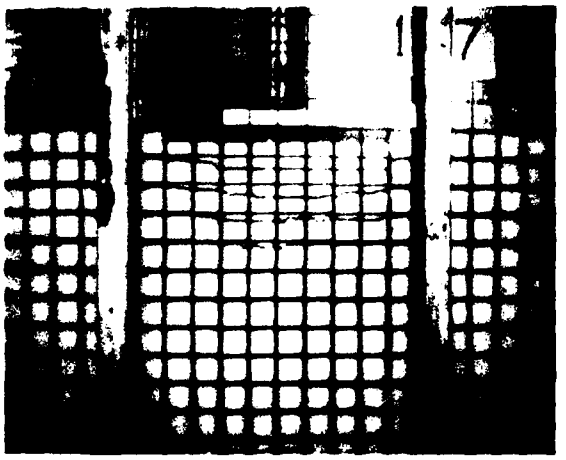

Figure 6. Results of laboratory study using a painted grid (Abele 1970).

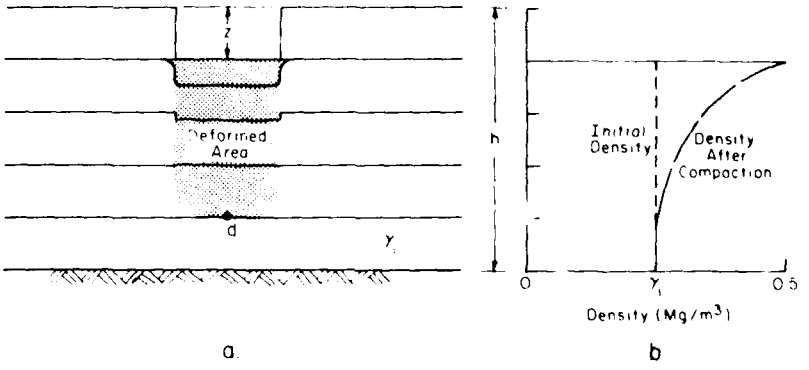

Figure 7. Representative schematic (a) and estimated density profile (b), z = sinkage, h = snow depth, γ_i = density, a = depth of deformation.

For eq 2 to be valid, the entire deformed area must be at the critical density. The equation thus requires a fully developed shallow snow case and does not take into account pressures which produce less than complete compaction (up to γ_{cr}) of the deformation area. However, the equation does define a sinkage depth where some other mechanism (such as plastic flow) must occur if a load larger than that required to produce z_e is applied. At this point it should be noted that the force-sinkage curve becomes asymptotic to sinkage = z_e (Fig. 5). Harrison (1975b) used this observation in his mobility calculations.

Throughout this discussion, all variables except load have been held constant in order to describe the mechanical behavior of the snow. It must

be realized that similar effects are obtained when a given load is applied to snows of varying depths and physical characteristics.

LABORATORY EXPERIMENT

Test Procedure

A laboratory experiment was conducted in order to obtain estimates of the terms T and S in eq 1. Load measuring devices were placed on top of a loading plate and on the "ground" surface to detect values of L and T. If a value of T could be measured before z_e was reached, then the deformed area extended to the base of the snow cover and its density could not be 0.5 Mg/m^3 throughout.

Test samples were prepared by placing a plywood box, 451 x 510 x 514 mm deep, in an Instron constant rate testing machine located in a -10°C coldroom. A load cell (Lebow model 3632) mounted in a fixture (Fig. 8) with dimensions similar to those of an M15 antitank mine (sensing plate diameter equal to 190.5 mm) was centered in the bottom of this box. Snow collected during the winter and stored at -15°C was sifted through a 5-mm mesh screen into the box. At depth intervals of approximately 50 mm, the snow was carefully leveled so that compaction would be minimized and a thin layer of blue chalk dust was placed on the snow to define the deformed area. The samples were prepared so that a total thickness of 178 to 250 mm of snow was above the sensing plate of the mine-simulating load cell. The samples were covered with plastic and allowed to age for 24 hours; one sample was aged 48 hours.

A load cell with a 204-mm-diam. loading plate was attached to the cross head of the testing machine. This plate diameter was chosen because

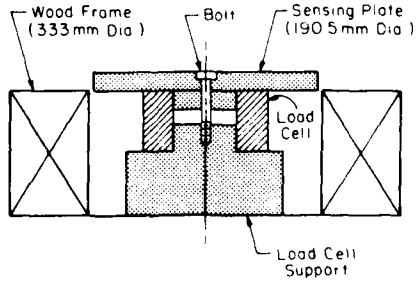

Figure 8. Cross section of load cell fixture, with outer dimensions similar to those of M15 antitank mine.

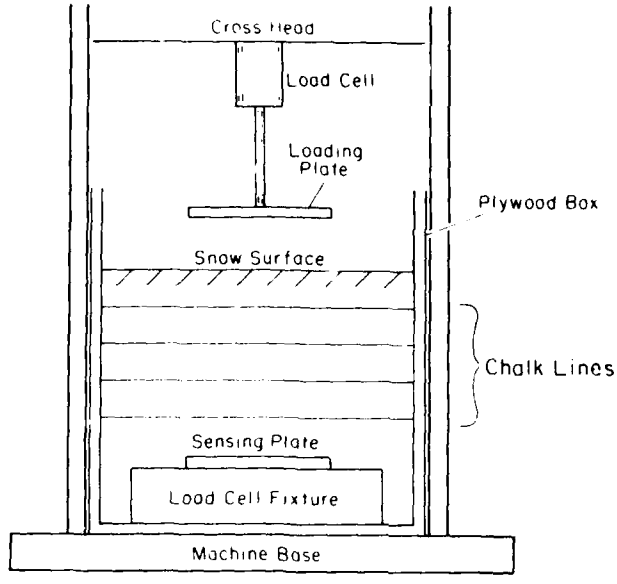

Figure 9. Test configuration.

Harrison (in prep.) has shown that edge effects are minimized at this or larger diameters. Figure 9 is a diagram of the complete test configuration.

After the sample was aged the desired length of time (24 or 48 hours), the testing machine was activated using the highest available loading rate, 50 mm/min. This rate is much slower than that produced by a moving vehicle, but it is assumed to be high enough so that the results would not appreciably differ. The output of the load cells was recorded on an x,y,y' plotter and simultaneously recorded on an instrumentation recorder. When the load measured by the upper load cell reached approximately 8800 N (2000 lbf), the test was stopped.

The sample was disassembled by removing the side of the box and half of the snow, as shown in Figure 10. Snow density measurements were obtained in the upper right-hand corner to provide initial density values. In some samples, density measurements of the deformed area were made, but the measurement results were questionable due to the size of the cylinder (used to obtain the snow density) relative to the deformed area. Measurements of sinkage and deformation were recorded and sketches and photographs of the deformed chalk lines made.

Results

Table 1 presents pertinent details of each test. A typical plot of

Figure 10. Photograph of sample 3 after disassembly.

load cell data is shown in Figure 11. The upper curve is the output of the loading plate and the lower that of the sensing plate. These are quite different from the bevameter results shown in Figure 5. This difference is due to the collapse mechanism of the snow and the stiffness of the loading apparatus, as discussed by Mellor (1975). In order to make analysis easier, the peak values of the load and corresponding sinkage were plotted (Fig. 12-17) for tests 3-8. Load vs sinkage data were not obtained for tests 1 and 2. The plot for test 4 is significantly different from the others, probably due to an instrumentation problem which necessitated stopping the test for several minutes after an initial load was applied.

As shown in Figure 10, placing layers of chalk dust in the snow accentuated the deformed area. The photograph from test 3 shows some bulging of deformed area, which can be explained by examining the load vs sinkage data for the test (Fig. 12). The load was increased until the

Table 1. Test data (all tests were conducted at -10°C).

Date (1980)	Test	Sample age(hr)	Initial density (Mg/m^3)	Depth (mm)	Sinkage (mm)	Force vs sinkage data
26 Jun	1	20	0.35	370	79.4	Lost*
27 Jun	2	20	0.34	340	44.4	Lost*
30 Jul	3	24	0.33	254	57	Figure 12
6 Aug	4	24	0.36	259	23	Figure 13+
7 Aug	5	24	0.38	216	57	Figure 14
8 Aug	6	24	0.39	184	57	Figure 15
13 Aug	7	48	0.39	190	76	Figure 16
14 Aug	8	24	0.40	190	89	Figure 17
3 Sep	9	24	--	514	--	--**

* Force-sinkage data lost due to instrumentation problem.

\+ Instrumentation problem, only limited questionable data were obtained.

** In this test the sample was constructed so that a vertical chalk line would indicate vertical displacement.

effective sinkage z_e was reached. Bulging then occurred as the sinkage, z, became greater than z_e.

Test 4 was stopped well before z_e was reached, and disassembly of this sample revealed no horizontal deformation. Tests 1 and 2 also showed no horizontal deformation.

The snow sample for test 9 was prepared with two vertical chalk lines extending through it in an attempt to ascertain the effect of horizontal deformation and the effect of the box sides. One line was approximately 100 mm from the box side, the other approximately 50 mm from the centerline

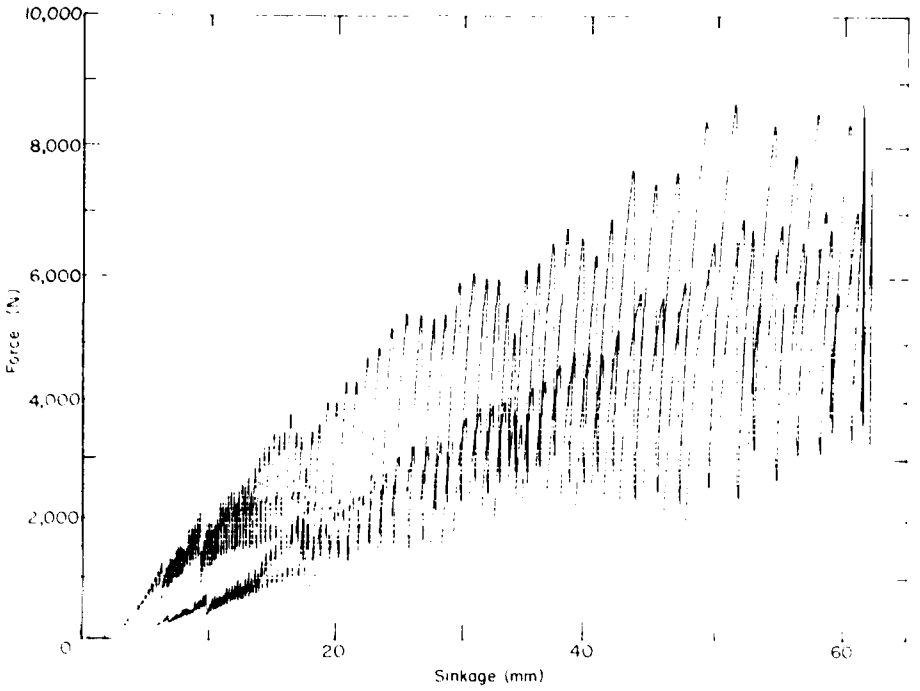

Figure 11. Typical load cell data.

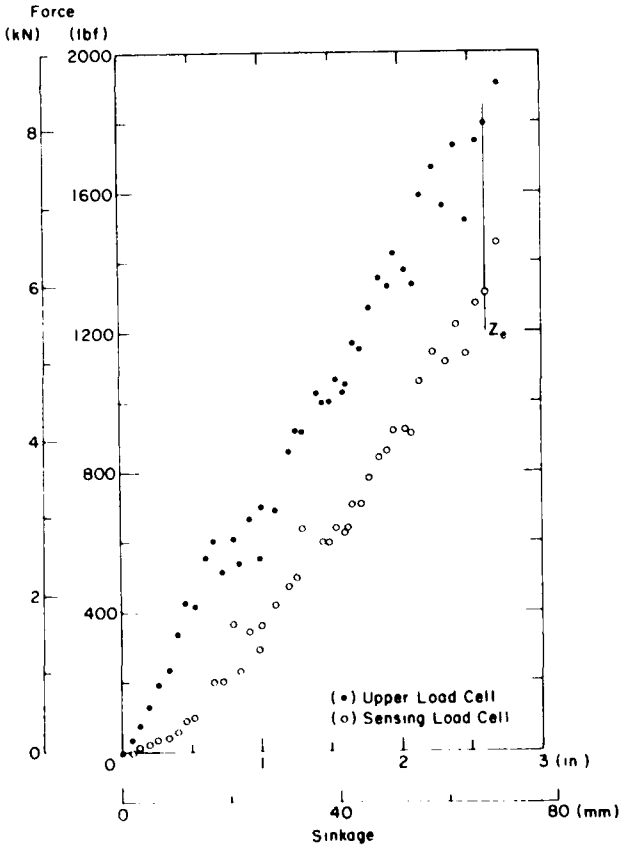

Figure 12. Force vs sinkage plot, test 3.

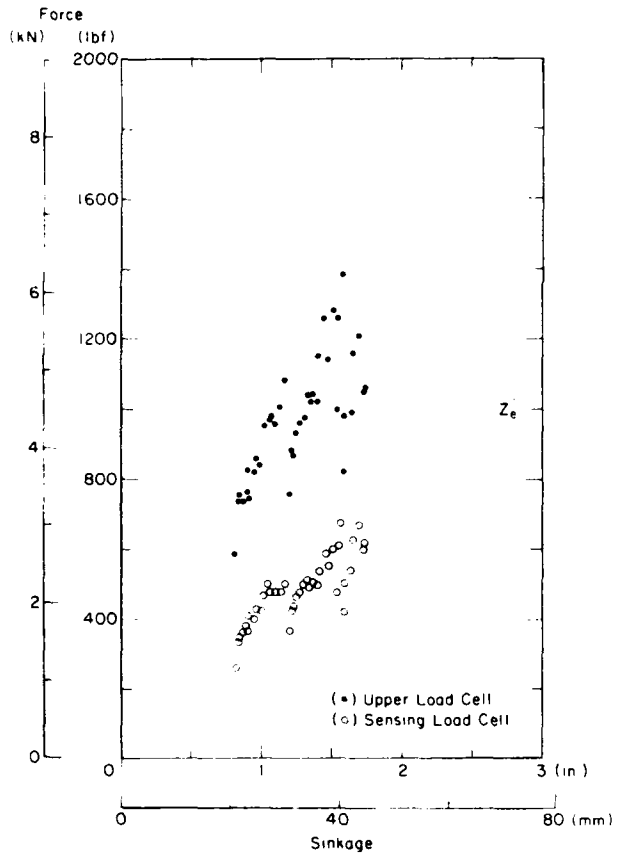

Figure 13. Force vs sinkage plot, test 4.

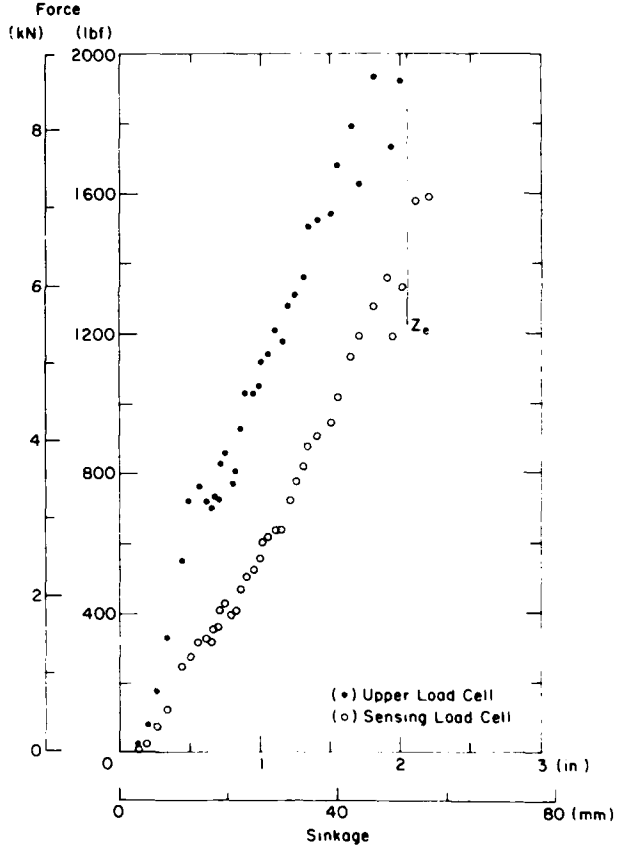

Figure 14. Force vs sinkage plot, test 5.

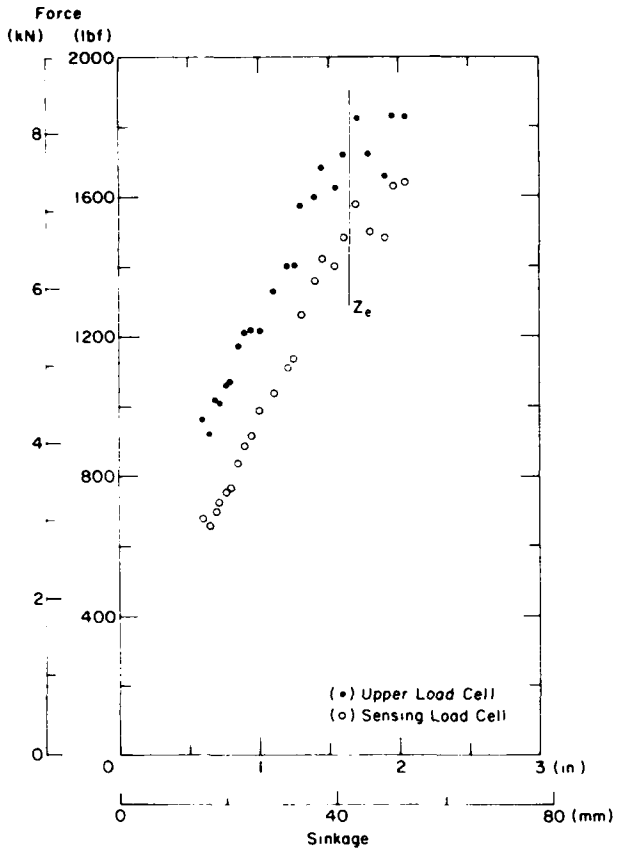

Figure 15. Force vs sinkage plot, test 6.

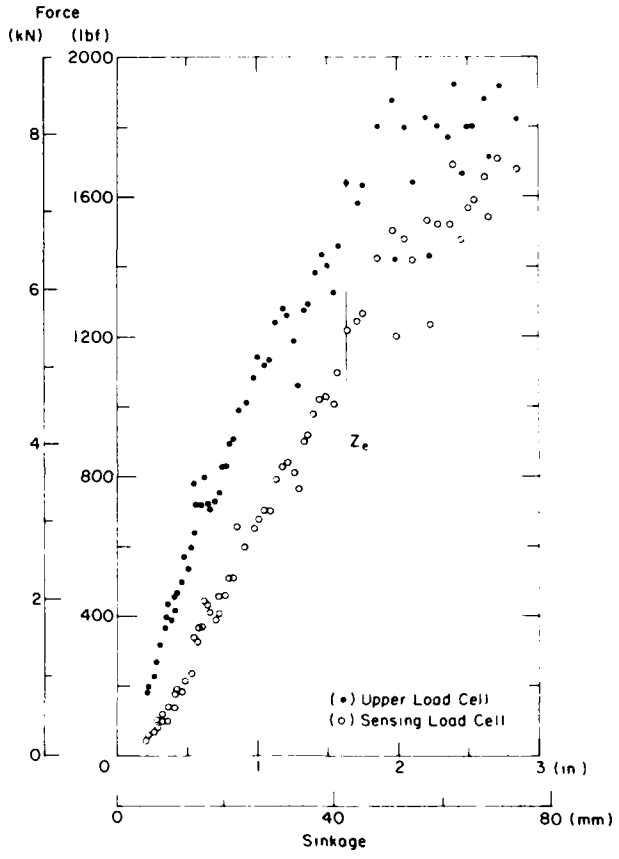

Figure 16. Force vs sinkage plot, test 7.

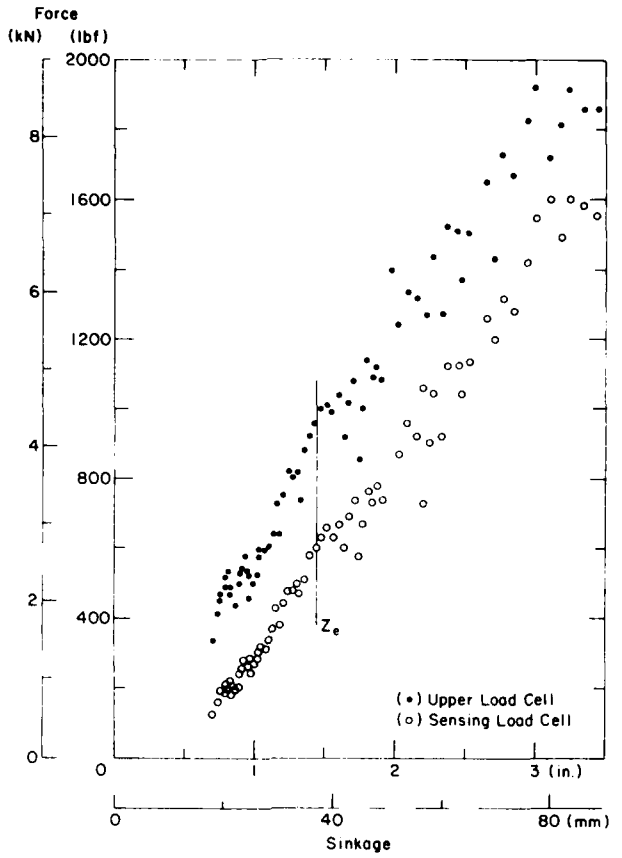

Figure 17. Force vs sinkage plot, test 8.

of the box. The snow depth was 514 mm with an initial density of 0.4 Mg/m^3. From eq 2, z_e is 104 mm, compared to a final sinkage of about 100 mm for test 9. Upon disassembly of the sample, no horizontal deformation was observed.

Analysis

Examination of the force vs sinkage plots (Fig. 12-17) reveals that the lower load cell began sensing a load almost immediately following the application of a load, indicating that the tests were in the shallow snow range. Since z_e had not been reached, these results support the observation that a density variation exists in the deformation bulb. The shape of the curves made by the data points is somewhat different from the in-situ curve shown in Figure 5, due perhaps to the density difference. No data for in-situ load-sinkage tests have been found in the literature for the density range of these tests.

It was believed that the curves would become asymptotic to a vertical

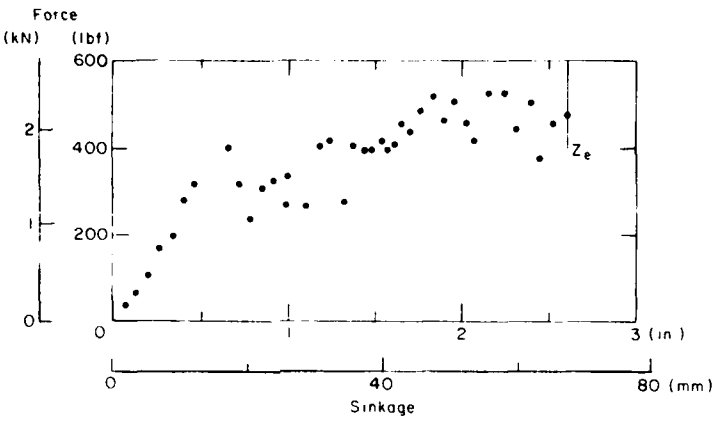

Figure 18. Force (S) vs sinkage plot, test 3.

line as the effective sinkage z_e was approached, this being the point where the average density in the deformed area would be 0.5 Mg/m^3. Examination of Figures 15-17 shows that this did not occur even when the effective sinkage was exceeded. These results suggest an ultimate strength of about 262 kPa (38 psi), which can be seen in Figure 16, near the end of this test. A curve suggested by the data points changes slope and then appears to level off at this value.

Figures 18-22 were prepared by taking the difference between corresponding data points of the upper and lower load cells on the force vs sinkage plots and plotting these with respect to sinkage. These data plots represent the value of S described earlier. In general, the maximum value of S occurs near the effective sinkage z_e and ranges from 1335 N (300 lbf) to 2670 N (600 lbf). If a cylindrical deformed volume of constant diameter under the upper loading plate is assumed, then the interfacial stress is found to have a maximum value of about 20.7 kPa (3.0 psi).

Two tests, 7 and 8, were continued well beyond the effective sinkage point. Plots of S for these two tests (Fig. 21 and 22) are significantly different after reaching z_e. In test 7, S decreased while in test 8 it remained relatively constant for about 38 mm of sinkage beyond z_e, before dropping off. Some bulging of the deformed area could have occurred in test 8 but not in test 7. The sample used in test 7 had aged 24 hours longer than the one in test 8 so that sample 7 was slightly stronger and more able to resist horizontal deformation.

With increasing sinkage, the interfacial force increases with the mobilization of snow crystals along the deformation interface until the

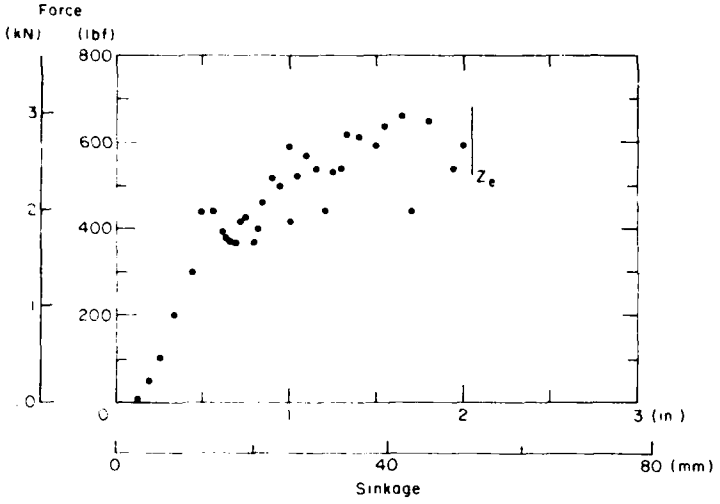

Figure 19. Force (S) vs sinkage plot, test 5.

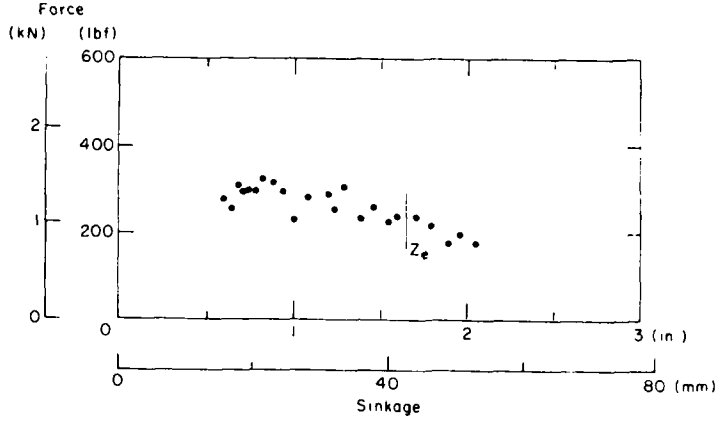

Figure 20. Force (S) vs sinkage plot, test 6.

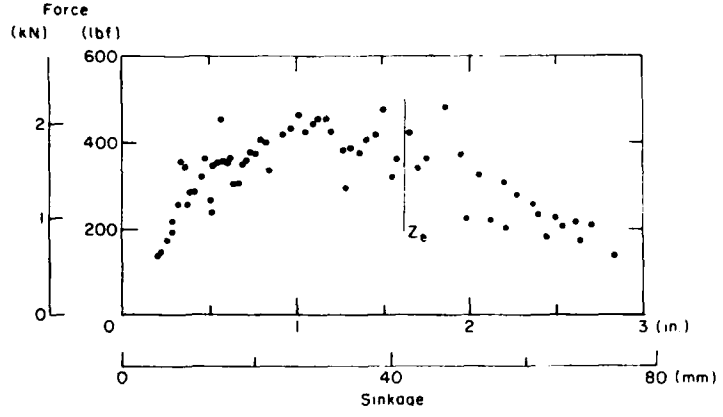

Figure 21. Force (S) vs sinkage plot, test 7.

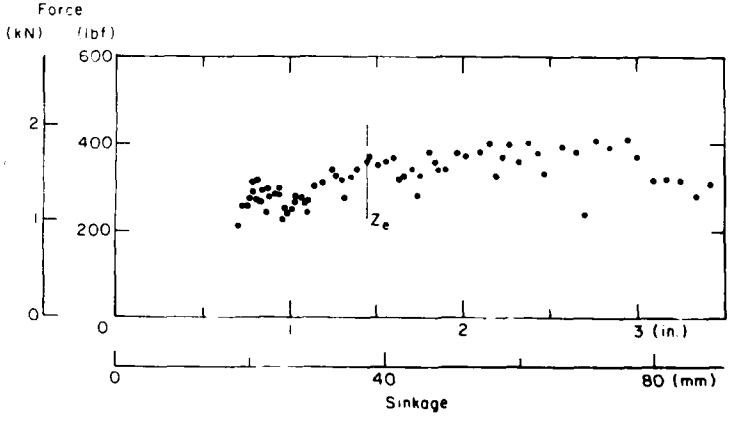

Figure 22. Figure (S) vs sinkage plot, test 8.

shallow snow case is reached. This increase in S is due to the increasing size (and thus surface area) of the deformation bulb. After this point, the boundary area begins to decrease (assuming that no lateral deformation takes place until the whole bulb is at γ_{cr}), suggesting that the interfacial force should also increase. This decrease in S is not observed in the results of these tests (Fig. 18-22); instead, the interfacial force continues to increase after the shallow snow case is reached, indicating that either the force normal to the interface is increasing or that the coefficient of friction is changing. It is reasonable to assume that the horizontal force is increasing as further deformation occurs and plastic yielding begins. There does not appear to be a reason for a change in the coefficient of friction.

APPLICATION

Vehicle Mobility

The performance of a vehicle traveling through snow is a function of the balance between the traction generated on the snow and the resistance to motion of the snow. At the point where the available tractive force is equal to the resistive force of the snow in front of the compacting wheels, the vehicle is immobilized when encountering any additional resistance. For predictive purposes, it is important to know the balance between these two opposing forces for a given snow condition and vehicle.

The amount of resistance to forward motion experienced by a vehicle is a function of the rut depth or vehicle sinkage z. It has been shown that sinkage is a result of the applied vertical load and the characteristics of the snow (both initial and final). Previous resistance estimates used the sinkage determined by eq 2, which is acceptable, provided that the vehicle ground pressure is adequate to give a sinkage of z_e and not so great that z_e is exceeded. Since eq 2 has no pressure term in it, it is not possible to know what sinkage a given vehicle will develop. The past assumptions were that normal vehicle ground pressures were large enough to create a sinkage of z_e. It was also felt that since the pressure-sinkage curve was asymptotic, overloading by a vehicle ($z > z_e$) was unlikely.

Table 2. Characteristics of U.S. Army pressure sensing anti-vehicle mines (U.S. Army 1977).

Nomenclature	Activation means	Activation force	Sensing plate diam.(mm)
M15, HE	pressure*	1.56 - 3.34 kN (350-750 lbf)	190
M19, HE, NM	pressure*	1.33 - 2.22 kN (300-500 lbf)	200
M21, HE	pressure* and or tiltrod	1.29 kN (290 lbf)	--+
M56**	pressure or anti-disturbance	unknown	unknown

* can also be booby trapped

\+ nearly a point load

** aircraft delivered.

The results of this work show that for some types of snow and vehicle combinations, these assumptions may not be valid. A tracked vehicle may well have a ground pressure which is not adequate to produce a sinkage of z_e. Use of eq 2 for this case will result in overestimating motion resistance. Likewise, a loaded wheeled vehicle may produce sinkages greater than z_e. If, as this work suggests, the force vs sinkage curve is not as exponential (approaching an asymptote) as previously thought, an underestimate of motion resistance could result.

An improved relationship between snow conditions (density, depth, compaction characteristics) and applied pressure is necessary. This relationship will allow more accurate determinations of vehicle mobility in snow.

Land Mines

Conventional anti-vehicle land mines require force on a pressure plate to cause activation. Currently there are four pressure sensing anti-vehicle mines in the U.S. Army inventory; their characteristics are shown in Table 2. A potential problem exists if these mines become covered

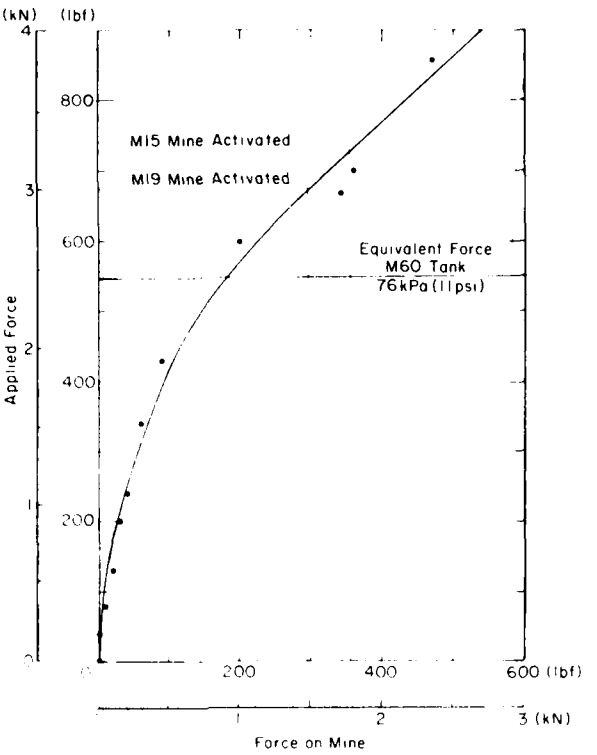

Figure 23. Mine activation plot, test 3 (snow depth = 254 mm, initial density = 0.37 Mg/m^3).

with snow. The presence of the interfacial force on the deformed snow area effectively attenuates the load applied so that a mine under the deformed area does not sense the entire applied load.

Data from tests 3 and 5 are plotted in Figures 23 and 24. As shown, the required activation loads (on the snow surface) for a snow-covered M15 and M19 mine are approximately 3.3 and 3 kN, respectively, under these snow conditions. These loads are higher than that applied by an M60 tank (Fig. 23 and 24) indicating that under these conditions (216 to 254 mm of snow overburden, 0.37 Mg/m^3 density, aged 24 hours) the M60 tank could safely pass over these mines.

Again, it must be pointed out that this represents only one snow condition; more tests and a greater understanding of the forces involved are required.

CONCLUSIONS

1. The deformed area under a vehicle is not of constant density, but

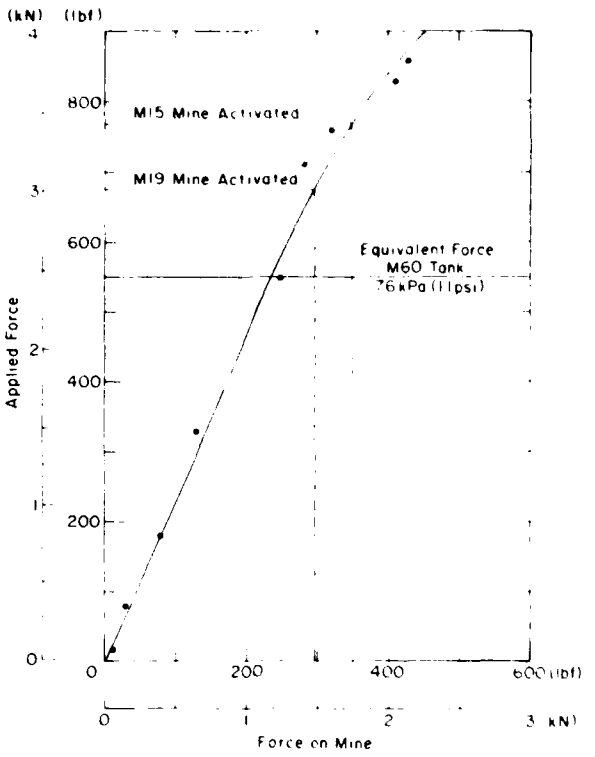

Figure 24. Mine activation plot, test 5 (snow depth = 216 mm, initial density = 0.38 Mg/m^3).

has some profile ranging from the initial density up to approximately 0.5 Mg/m^3, the critical density

2. A laboratory test was developed which allows the deformed area to be examined after applied and transferred load measurements are made.

3. The applicability of this work to military engineering has been shown. Land mine sensitivity is effectively degraded for the snow conditions tested. Prediction of vehicle motion resistance based on a sinkage value calculated from eq 2 is shown to apply only to a select few cases where the vehicle ground pressure and snow type combine to yield a final snow density of 0.5 Mg/m^3.

RECOMMENDATIONS

1. A method of measuring the density distribution of deformed snow needs to be developed.
2. Tests must be done to further evaluate the effect of a snow cover on land mines.

3. An improved relationship between applied pressure, snow density (initial and final) and snow depth needs to be developed to predict sinkages.

LITERATURE CITED

Abele, G. (1970) Deformation of snow under rigid plates at a constant rate of deformation. CRREL Research Report 273, AD 704708.

Bennett, W.D. (1973) Documentation of snow characteristics for over-snow vehicle validation tests. CRREL Technical Note (unpublished).

Blaisdell, G.L. (in prep.) Predicting vehicle motion resistance in shallow snow. CRREL Special Report in preparation.

Gensler, R.E. (1973) Land mine and countermine warfare, Western Europe, World War II. Engineer Agency for Resource Inventories, Washington, D.C.

Harrison, W.L. (in prep.) Shallow snow model for predicting vehicle performance. CRREL Report in preparation.

Harrison, W.L. (1975a) Vehicle performance over snow: Math-model validation study. CRREL Techinal Report 268, ADA021228.

Harrison, W.L. (1975b) Shallow snow performance of wheeled vehicles. In Proceedings, 5th International Conference of the International Society for Terrain-Vehicle Systems, June 2-6, Detroit, MI, Vol. 2, p. 589-614.

Mellor, M. (1975) A review of basic snow mechanics. International Association of Scientific Hydrology Publication no. 114, p. 251-291.

U.S. Army (1977) Army ammunition data sheets for land mines (FSC 1345). Technical Manual TM 43-0001-36.

Wuori, A.F. (1962) Supporting capacity of processed snow runways. CRREL Technical Report 82, AD 414995.